JOURNAL OF Materials CHEMISTRY

Sol–gel synthesis *via* an aqueous semi-alkoxide route and characterization of zircon powders

Christelle Veytizou,[a] Jean-François Quinson[a] and André Douy[b]

[a]*Laboratoire GEMPPM, UMR CNRS 5510 INSA, 20 Avenue Albert Einstein, 69621 Villeurbanne Cedex, France*
[b]*CNRS – Centre de Recherches sur les Matériaux à Haute Température, 1d Avenue de la recherche scientifique, 45071 Orleans Cedex 2, France*

Received 26th July 1999, Accepted 20th October 1999

The synthesis of zircon powders from an aqueous precusor sol has been studied. The starting solution, prepared by hydrolyzing TEOS in an aqueous solution of zirconyl nitrate, was refluxed then precipitated into an ammonia solution. The evolution of the precursor sol with reflux time and that of the precursor powder, *i.e.* the precipitate dried and ground, with heat treatment has been followed by several characterization techniques, *viz.* Raman spectroscopy, ^{29}Si MAS NMR spectroscopy, X-ray diffraction and DTA–TGA analysis. It was found that zircon formation begins at 100 °C in the refluxing precursor sol and is carried on into the precursor powder by reaction between amorphous silica and tetragonal zirconia, formed earlier during the heat treatment at temperatures above 1000 °C. A procedure for the preparation of zircon powders consisting of dense spherical particles based on spray-drying of the precipitate, washed and re-dispersed in water after synthesis, is also described.

I Introduction

Zircon, $ZrSiO_4$, is the only crystalline phase in the binary SiO_2–ZrO_2 system that is stable under 1676 °C. This oxide exhibits low thermal expansion, low thermal conductivity, and high resistance to thermal shock. To take advantage of such properties, which are very interesting for high temperature applications, the zircon should be highly pure. Indeed, impurities such as Al_2O_3, Fe_2O_3, TiO_2 and SiO_2, found in natural zircon sand, can lead to a lowering of its decomposition temperature and alteration of its mechanical properties.

Although difficult, the preparation of high-purity $ZrSiO_4$ has already been the subject of a great number of research papers. Various different synthetic routes have been investigated. The formation of zircon powders at temperatures as low as 150 °C is possible under hydrothermal conditions.[1–3] Sol–gel processing has also been used by combining numerous precursors in aqueous or organic media, including sols, salts and alkoxides.[4–18] In this case, literature data indicate that pure zircon is produced at high temperatures varying between 1100–1500 °C according to the procedure followed. However, Mosset *et al.*[2] have shown that partially crystallized zircon can be formed at 100 °C.

The present paper discusses zircon synthesis by a new aqueous semi-alkoxide route, combining tetraethoxysilane (TEOS) with zirconyl nitrate $ZrO(NO_3)_2{\cdot}xH_2O$: an aqueous solution of zirconyl nitrate in which TEOS has been hydrolysed into silicic acid constitutes a homogeneous zircon precursor. A procedure for the preparation of spherical $ZrSiO_4$ particles from the starting precursor solution is also described, which is of interest considering that methods for obtaining pure zircon powders with controlled morphology have scarcely been mentioned in the literature to date.

II Experimental

II-1 Synthesis

Zircon powders were prepared using as starting precursors, tetraethoxysilane (TEOS) $Si(OC_2H_5)_4$ (Aldrich; no 33,385-9) and zirconyl nitrate $ZrO(NO_3)_2{\cdot}xH_2O$ with $x \approx 6$ (Aldrich; no 24,349-3), the exact x value being determined by thermogravimetry for each batch of commercially obtained nitrate. Zirconyl nitrate was firstly dissolved in water and TEOS added in a stoichiometric ratio with vigorous stirring. Afterwards, when the precursor solution became clear, it was treated under reflux at 100 °C for at least 24 h and then added with stirring to a dilute aqueous ammonia solution (≈1% vol.). A colloidal precipitate was immediately formed which was filtered off and washed several times with deionized water in order to eliminate as much ammonium nitrate resulting from the reaction as possible. Then, after oven-drying overnight at 100 °C and grinding with an agate mortar and pestle, the precipitate was transformed into the precursor powder.

Different precursor amounts, corresponding to concentrations in zircon varying from 0.10 to 0.20 mol l^{-1}, were tested for the preparation of the powders. It was noted that the temperature for which the full transformation to zircon occurs depended on the concentration of the starting solution: its lowest value, about 1150 °C, was reached for a precursor solution corresponding to a concentration of zircon of 0.12 mol l^{-1} only. Consequently, this solution was chosen to prepare the zircon powders under study.

II-2 Characterization methods

The reaction mixture was monitored at various stages from the sol state to the calcined solid using several techniques.

In order to investigate the extent of the hydrolysis–condensation reaction and the nature of the species formed during the treatment under reflux, Raman spectroscopy was used. Raman scattering was excited by the 514 nm radiation of an Ar^+ ion laser, and spectra were taken on a Dilor XY microspectrometer.

The elimination of water and the combustion of residual species contained in the dried powders were examined by differential thermal analysis (DTA) coupled with thermogravimetric analysis (TGA). DTA–TGA measurements were made in air at a scan rate of 300 °C h^{-1}.

The granulometric distributions of the powders were

obtained using a laser size analyser, their specific surface area was evaluated by the BET nitrogen adsorption method, and their morphology was observed by scanning electron microscopy (SEM). The structural evolution was both followed by X-ray diffraction (XRD) using Cu-Kα radiation, and by ^{29}Si and ^{29}Si–^{1}H CP MAS NMR spectroscopy on a Bruker DSX 300 operating at 7 T. The ^{29}Si MAS spectra, recorded with a 10 kHz spinning rate using a single pulse ($\pi/10$) excitation, are the sum of 3600 transients acquired with a recycle delay of 15 s. It should be noted that the recycle delay and pulse length were optimised to allow a quantitative NMR analysis. The ^{29}Si–^{1}H cross polarization (CP) MAS experiments were performed with a spinning rate of 5 kHz, using a contact time of 5 ms. The ^{1}H $\pi/2$ pulse duration was 5.3 μs and the recycle delay was set to 2 s. ^{29}Si chemical shifts are referenced to tetramethylsilane (TMS).

The apparent crystallite size, D, was estimated from the TEM micrographs, and calculated from the XRD data using the Laue–Scherrer formula:

$$D = K\lambda/\beta\cos\theta$$

with $K=1$,[19] where λ is the Cu-Kα wavelength and θ the diffraction peak angle. β measured in radians, corresponds to the half-width of the diffraction peak; it is taken as the experimental half-linewidth (β_{exp}) and was corrected for experimental broadening (β_{instr}) according to the relation:

$$\beta^2 = (\beta_{exp}{}^2 - \beta_{instr}{}^2)$$

β_{instr} was determined experimentally on the (101) diffraction peak of a highly pure quartz sample composed of large crystallites.

III Results and discussion

III-1 Synthesis

Zircon was synthesised from zirconyl nitrate and TEOS through an aqueous route. The use of TEOS in an aqueous medium is rather unusual. The use of alcohol as the common solvent for the nitrate and TEOS is not necessary. Although TEOS is not directly miscible with water, it is rapidly hydrolysed under stirring and acid catalysis from the solution of zirconyl nitrate. This reaction occurs in less than half an hour and a clear solution is obtained. For an equivalent concentration of 0.12 mol l^{-1} of zircon, the molar ratio [H_2O]/[TEOS] is high and approximately equal to 450: it is therefore assumed that TEOS is initially completely hydrolysed into silicic acid $Si(OH)_4$. Under these conditions, the aqueous route leads to a reactive precursor solution of zirconyl nitrate and silicic acid. This approach is very attractive because the silicic acid is formed *in situ* and not, for example, from water-soluble silicates in which metallic ions have been exchanged for H^+ on a cation-exchange resin.

Moreover, the fact that the precursor solution treated under reflux was turning opalescent after a few hours reveals an evolution. The simplest method found for collecting the species formed for characterization and thermal treatment was to precipitate the sol into an ammonia solution. During this step, the hydrolysis of zirconium is completed and the colloidal species are condensed. The precipitate may then be easily filtered off, washed with water and dried.

It is known that colloidal silica is soluble in ammonia solutions, and more generally in alkaline media, hence no precipitate is formed when adding a solution of silicic acid alone [prepared by hydrolysing TEOS at the same concentration and the same pH (nitric acid)] into an ammonia solution. On the contrary, in the presence of zirconyl nitrate, all the siliceous species were precipitated into the ammonia solution, and this even though the precipitation was carried out before refluxing: indeed, no trace of silicon was detected in the filtrate after concentrating and neutralising, since silica displays minimal solubility in aqueous solutions at neutral pH.[20]

III-2 Sol characterization

Because of the high dilution of the starting solution used for synthesising zircon, it was not possible from IR, Raman and ^{29}Si NMR analyses performed on the sols themselves, to identify the species formed after refluxing. However, after evaporation of the sols at 100 °C in order to eliminate water and ethanol generated *in situ* during TEOS hydrolysis–condensation, useful data were obtained. Although the solid residues obtained in this manner, and studied by Raman spectroscopy, are not exactly in the same state as in the colloidal sol, since condensation reactions may occur during the drying step, the evolution with reflux time observed on the dried samples should be characteristic of the evolution inside the sol.

Raman spectra of gels resulting from the evaporation of two solutions treated, respectively, under reflux for 24 and 48 h are shown in Fig. 1a, b.

Analysis of these spectra reveals:

on one hand, the presence of bands due to the zirconium precursor (Fig. 2); those at 709 and 767 cm^{-1} are not assigned, the others at 576, 1052, and 1032 cm^{-1} are generated by vibrational motions involving Zr–O bonds,[21] NO_3^- groups,[22,23] and Zr–OH bonds, respectively. This last assignment is consistent with the fact that the intensity of the Raman band at 1032 cm^{-1} increases strongly during the reflux treatment, then decreases with reaction time.

on the other hand, the appearance of two new bands in the 950–1010 cm^{-1} range, whose intensities increase with the reflux time. It is obvious that the band at 1006–1007 cm^{-1} can be identified with the principal peak detected in the Raman spectrum of zircon obtained by calcining the precursor powder at 1300 °C (Fig. 3). The other band, situated at about

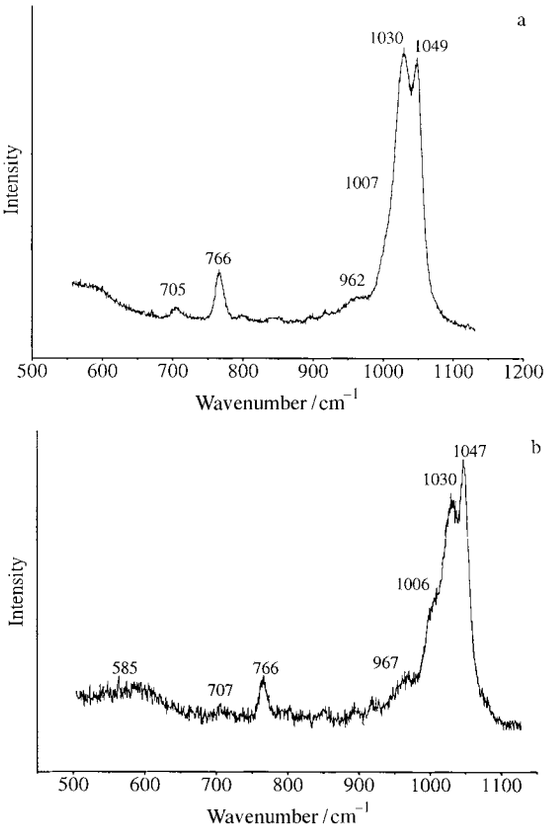

Fig. 1 Raman spectra of solutions refluxed for 24 h (a) and 48 h (b).

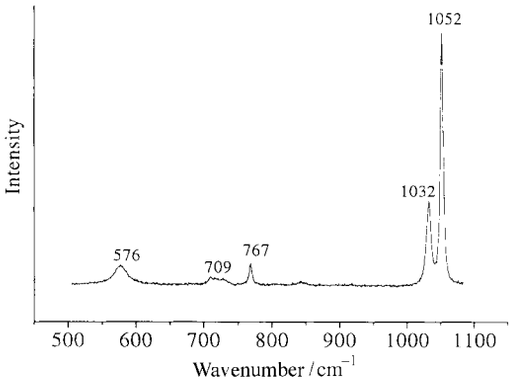

Fig. 2 Raman spectrum of zirconyl nitrate, $ZrO(NO_3)_2 \cdot xH_2O$.

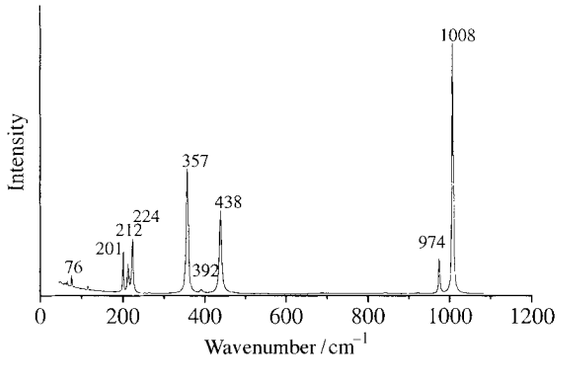

Fig. 3 Raman spectrum of $ZrSiO_4$ obtained by calcining the precursor powder at 1300 °C.

965 cm^{-1}, is assumed to correspond to Zr–O–Si bonds and/or Si–OH linkages.[21,24]

III-3 Powder characterization

X-Ray and ^{29}Si MAS NMR characterization of the precursor powder, obtained after drying (at 100 °C) of the precipitate formed from a solution refluxed for 24 h, confirms the presence of the zircon network at low temperature. Indeed, the XRD pattern of this powder (Fig. 4a) reveals that a lot of the zircon is already partially crystallized.

The same conclusion can be deduced from the ^{29}Si MAS NMR spectrum of the sample (Fig. 4b); a sharp peak at −82.0 ppm corresponding to the single Si site in zircon[18,25–26] is detected, in addition to a broad band centered at −91.5 ppm. The latter is assumed to be the superposition of several signals assigned to various Si sites, Q_x, where x refers to the number of siloxane bonds surrounding the Si atom.[26] These sites could both be associated with some partly hydroxylated species and chemical environments such as $Si(OSi)_2(OZr)_2$ and $Si(OSi)(OZr)_3$.

The influence of the precursor solution reflux time on the zircon yield of the resulting precursor powder was followed by NMR. Both ^{29}Si MAS and ^{29}Si–^{1}H CP MAS spectra were recorded (Fig. 5). ^{29}Si–^{1}H CP MAS spectra exhibit a better resolution and can be simulated by two components assuming Gaussian line shapes. Yet, this ^{29}Si–^{1}H coupling spectroscopy does not allow a precise quantification of all Si sites, the contact time being optimum only for Q_2. On the contrary, both the relative amounts of the zircon and siliceous phases were accurately calculated from ^{29}Si MAS spectra simulated in the same way as the ^{29}Si–^{1}H CP MAS spectra. These data (I) as well as the chemical shift (δ) and the full width at half maximum (Fwhm) of two peaks observed in the simulated ^{29}Si MAS spectra are given in Table 1.

Concerning the siliceous phase, the evolution of δ and Fwhm suggests an increase in the degree of condensation species with reflux time. As for zircon, while the variation of the Fwhm is not significant, its yield in the precursor powder increases with reflux time and reaches 39% after 6 days. This last result means, in fact, that the amount of Zr–O–Si species formed in the sols, although apparently limited, depends on reflux time.

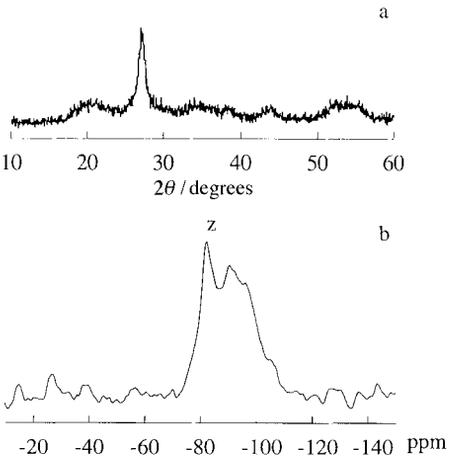

Fig. 4 XRD (a) and ^{29}Si MAS NMR (b) spectra of a precursor powder obtained from a sol refluxed for 24 h. z = zircon.

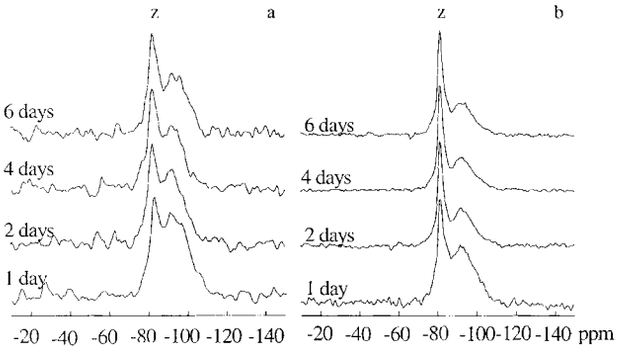

Fig. 5 ^{29}Si MAS (a) and ^{29}Si–^{1}H CP-MAS NMR (b) spectra of precursor powders obtained from sols refluxed for different lengths of time.

Table 1 ^{29}Si MAS NMR spectra modelling[a]

	Zircon			Siliceous phase		
Reflux time/days	δ	Fwhm	I (%)	δ	Fwhm	I (%)
1	−82	4.4	15.2	−92	18.2	84.8
2	−81.7	4.8	19.9	−92.6	16.6	80.1
4	−82	4.7	34.1	−91.5	13.5	65.9
6	−82	4.0	39.3	−93.2	15.3	60.7

[a] $\delta \pm 0.3$ ppm, Fwhm ± 1 ppm, $I \pm 5\%$.

III-4 Thermal treatment effect

The thermal behaviour of the precursor powder, obtained from a sol refluxed for 24 h, was studied in an air atmosphere up to 1300 °C by differential thermal and thermogravimetric analyses (DTA–TGA), X-ray diffraction (XRD), and Raman spectroscopy. The DTA–TGA traces, recorded at a scan rate of 300 °C h^{-1}, are illustrated in Fig. 6.

The DTA curve shows two endothermic peaks below 200 °C which correspond to the weight loss in the TGA curve caused by successive desorption of free and physically adsorbed water. Beyond 200 °C and up to around 400 °C, a broad exothermic peak associated with a weight loss is observed. This peak is assigned to the decomposition of ammonium nitrate still present in the colloidal precipitate after rinsing with water. At

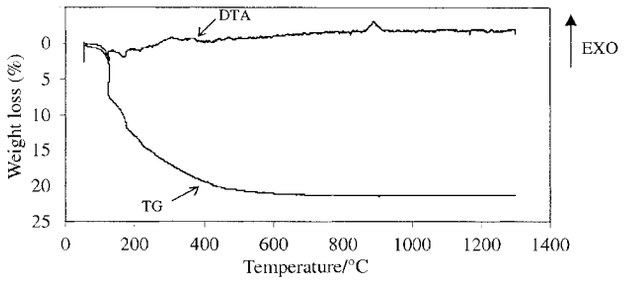

Fig. 6 DTA and TGA curves, in an air atmosphere and with a scan rate of 300 °C h^{-1}, of the precursor powder obtained from a sol refluxed for 24 h.

higher temperatures, while the weight loss apparently ends at 600 °C, a sharp exothermic peak is observed at about 900 °C in the DTA curve.

The evolution of the X-ray diffraction patterns of the precursor powder (Fig. 7), heated at a rate of 300 °C h^{-1} to the desired temperature in the range 600–1300 °C, then cooled to room temperature by quenching in air, suggests that this exotherm is due to crystallisation of amorphous zirconia (a-ZrO_2) into the tetragonal phase (t-ZrO_2). Indeed, on heating, a broadened XRD peak at $2\theta = 30.2°$, characteristic of t-ZrO_2, is detected. The peak intensity increases with temperature indicating an improvement in the crystallinity of the t-ZrO_2. Partially crystallised zircon, detected from 100 °C, is always present at 1300 °C but the intensity of the diffraction peak is still very low. Yet, under suitable calcining conditions (Table 2), as determined from the X-ray diffraction patterns of the precursor powder subjected to isothermal firings in the temperature range 1150–1300 °C, single phase zircon was obtained.

As shown in Table 2, the duration of the synthesis can be relatively brief compared with other zircon syntheses found in the literature: for example, from a sol refluxed for 24 h, the full synthesis of zircon can be achieved in less than a day, when the precursor powder is calcined at 1300 °C. It is also noted that the crystallite size of $ZrSiO_4$ does not significantly vary with calcination temperature. Its value, estimated at around 50 nm, is confirmed by the TEM micrograph of the zircon obtained by calcining the precursor powder at 1300 °C (Fig. 8).

The structural evolution of the precursor powder after calcination at different temperatures for 1 h, followed by both XRD analysis and ^{29}Si MAS NMR spectroscopy, produces

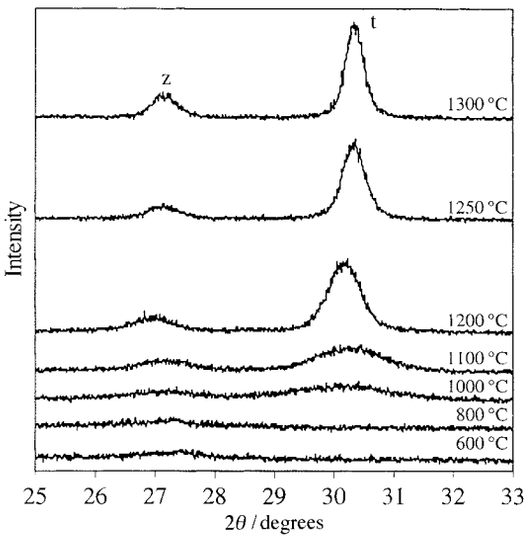

Fig. 7 XRD patterns of the precursor powder heated up to various temperatures in the range 600–1300 °C, then cooled to room temperature by quenching in air. t = tetragonal zirconia; z = zircon.

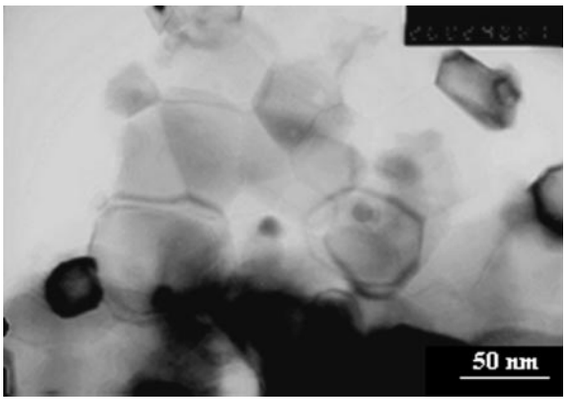

Fig. 8 TEM micrograph of $ZrSiO_4$ obtained by calcining the precursor powder at 1300 °C.

Table 2 Calcination temperatures and holding times for which only the zircon phase is obtained

Temperature/°C	1150	1200	1250	1300
Holding time/h	18	4	1¼	¼

evidence that almost all the zircon is formed by the reaction of tetragonal zirconia with amorphous silica, with a low yield already being generated under reflux. Indeed, from 1000 °C onwards the XRD patterns (Fig. 9a) clearly reveal the presence of tetragonal zirconia, which afterwards disappears at 1300 °C as a result of its full transformation to zircon. In the same way, the broad band around −110 ppm due to amorphous silica,[27] observed in the ^{29}Si MAS NMR spectra (Fig. 9b), is no longer detected.

It is worth noting that no obvious signal due to zircon formation is observed at high temperature in the DTA curve (Fig. 6), which could be explained by the transformation mechanism propounded by Itoh:[13] SiO_2 dissolution into ZrO_2

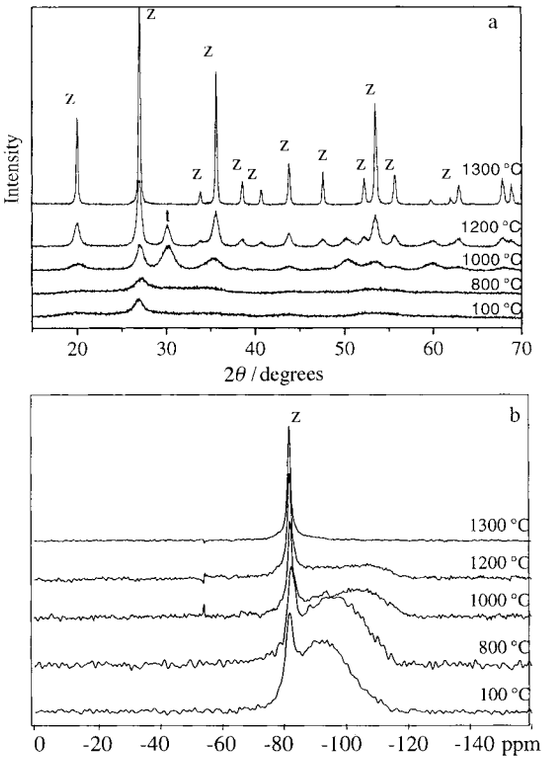

Fig. 9 XRD patterns (a) and ^{29}Si MAS NMR spectra (b) of the precursor powder after heating at different temperatures for 1 h. z = zircon; t = tetragonal zirconia.

to form a solid solution with the crystal structure of t-ZrO_2, which is then converted to $ZrSiO_4$.

III-5 Particle morphology

SEM examination of the precursor powder prior to calcination (Fig. 10a) showed both irregularly shaped and differently sized agglomerates or aggregates. The granulometric analysis determined a broadened volume particle-size distribution, varying from 0.1 to 800 μm (Fig. 11a). This curve only exhibits a slight shift toward the lowest sizes after successive treatment in a high speed homogenizer (ultra-turrax apparatus) and in an ultrasonic cell of the precursor powder re-dispersed in water. In view of this result, the large particles observed are related to aggregates probably resulting from rinsing with water carried out in order to eliminate ammonium nitrate formed during sol precipitation.

Particle size, distribution, and shape being important factors for the densification of ceramic powders, a method of preparing zircon powders with controlled morphology has been developed. In this case, after washing, the colloidal precipitate is not oven dried at 100 °C, but is re-dispersed in water under vigorous stirring, then spray-dried. The spray-drying experiments were performed under a flow of dry air maintained at 140 °C, using a Buchi 190 mini spray drier equipped with a 0.5 mm diameter nozzle. This atomizer operates on the principle of nozzle spraying in parallel flow, *i.e.* the sprayed product and the drying air flow in the same direction.

SEM micrographs of the precursor powder produced by spray-drying (Fig. 12a) show that the particles are spherical in shape, as expected. Moreover, the particles are unagglomerate and the largest do not exceed 10 μm in size.

The volume particle-size distribution (Fig. 13a) is symmetrical and not very broad, particle diameters ranging from 0.2 to 10 μm. The volume mode diameter, d_{max}, and the volume median diameter, d_{50}, equal to 1.78 and 1.84 μm, respectively, are practically coincident.

Calcination treatment at 1300 °C does not modify the dried powder morphology, as shown by SEM micrographs illustrated in Fig. 10b and 12b: the particles remain as spheres or as irregularly shaped aggregates according to the drying procedure used. On the other hand, the granulometric analysis indicates bimodal particle size distributions (Fig. 11b and 13b), as well as a decrease in particle size, which is clearly larger in the case of previously oven-dried powders. Finally, the drastic

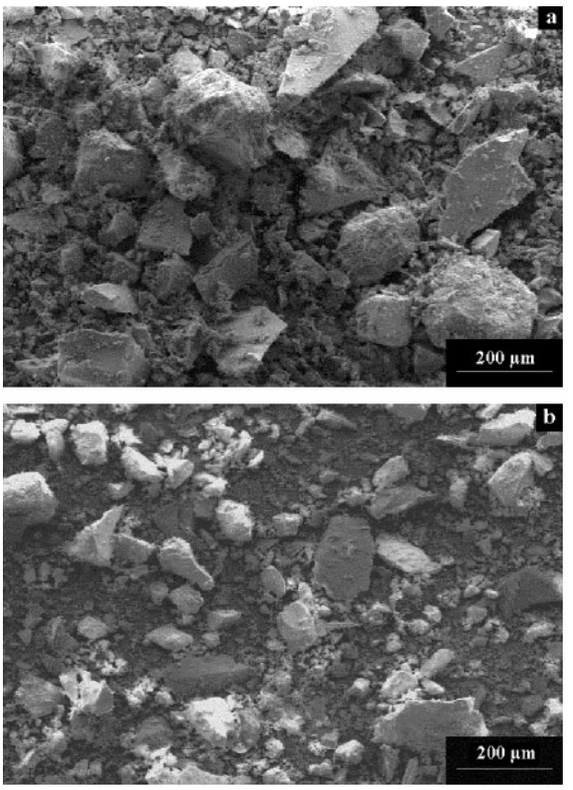

Fig. 10 SEM micrographs before (a) and after (b) calcination at 1300 °C of the powder obtained by oven-drying.

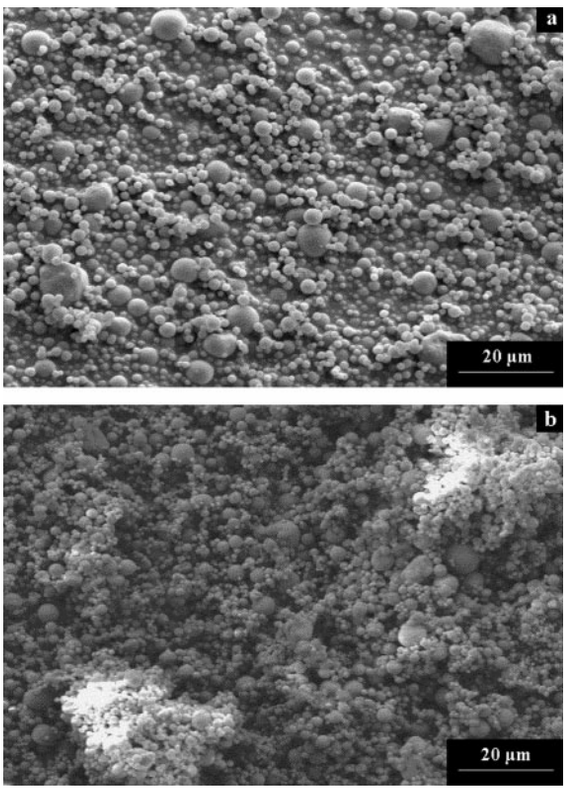

Fig. 12 SEM micrographs before (a) and after (b) calcination at 1300 °C of the powder produced by spray-drying.

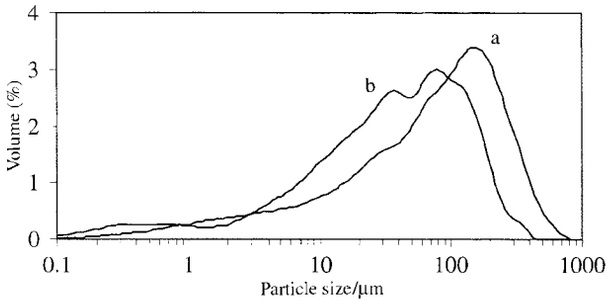

Fig. 11 Particle size distribution before (a) and after (b) calcination at 1300 °C of the powder obtained by oven-drying.

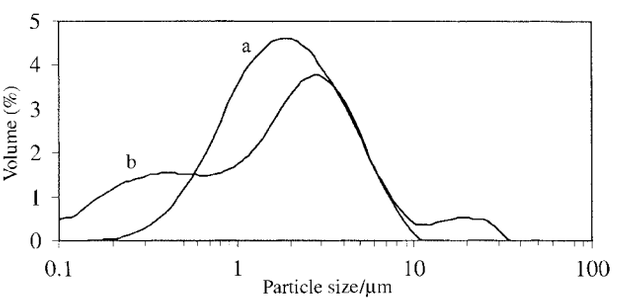

Fig. 13 Particle size distribution before (a) and after (b) calcination at 1300 °C of the powder produced by spray-drying.

Table 3 Specific surface areas of dried and calcined powders

Sample	Specific surface area/$m^2\ g^{-1}$	
	Before calcination	After calcination
Oven-dried powder	412	~1
Spray-dried powder	362	~1

decrease of the BET surface areas observed after calcination (Table 3) denotes a high densification of the particles.

It is worth noting from Table 3 that the specific surface areas of the differently dried, uncalcined powders are dissimilar. This result is probably due to a higher drying temperature in the spray-dryer than in an oven. The drying procedure does not seem to influence this variation. Likewise, it does not affect the structural evolution of dried powders during thermal treatment; pure zircon is always formed, even at relatively low temperatures.

IV Conclusion

Sol–gel processing *via* an aqueous semi-alkoxide route, combining zirconyl nitrate and tetraethoxysilane, has been found to be an excellent technique for the synthesis of zircon. Zr–O–Si bonds are formed *in situ* when the starting solution is heated to reflux at 100 °C. The resulting zircon yield detected in the colloidal precipitate (obtained by adding ammonia to the refluxed precursor solution), although apparently limited, can increase up to 39% for a reflux time of 6 days.

The structural evolution of the precursor powder, *i.e.* the precipitate dried then ground, with heat treatment reveals that the entire transformation to zircon, possible from 1150 °C, proceeds by reaction between unreacted amorphous silica and tetragonal zirconia. This reaction apparently takes place as soon as the amorphous zirconia is crystallized into the tetragonal structure.

Another attractive aspect of the present work is that it has been shown that zircon powders consisting of dense spherical particles can be produced by spray-drying and calcination at high temperature.

Acknowledgements

The authors wish to thank Dr. F. Fayon (CNRS-CRMHT, Orléans) for performing NMR measurements, and Région Rhône-Alpes for financial support.

References

1 S. Komarmeni, R. Roy and Q. H. Li, *Mater. Res. Bull.*, 1992, **27**, 1393.
2 A. Mosset, P. Baules, P. Lecante, J. C. Trombe, H. Ahamdane and F. Bensamka, *J. Mater. Chem.*, 1996, **6**, 1527.
3 R. Valero, B. Durand, J. L. Guth and T. Chopin, *J. Sol–Gel Sci. Technol.*, 1998, **13**, 119.
4 M. Nogami, *J. Non-Cryst. Solids*, 1985, **69**, 415.
5 N. Nogami and M. Tomozawa, *J. Am. Ceram. Soc.*, 1986, **69**, 9.
6 Y. Kanno and T. Suzuki, *J. Mater. Sci. Lett.*, 1988, **7**, 386.
7 Y. Kanno, *J. Mater. Sci.*, 1989, **24**, 2415.
8 J. Campaniello, E. M. Rabinovich, P. Berthet, A. Revcolevschi and N. A. Kopylov, *Mater. Res. Soc. Symp. Proc.*, 1990, **180**, 541.
9 S. S. Jada, *J. Mater. Sci. Lett.*, 1990, **9**, 565.
10 M. Salvado and F. Navarro, *J. Mater. Sci. Lett.*, 1990, **9**, 173.
11 H. Kobayashi, T. Terasaki, H. Yamamura and T. Mitamura, *Seramikkusu Ronbunshi*, 1991, **99**, 42.
12 T. Mori, H. Yamamura, H. Kobayashi and T. Mitamura, *J. Am. Ceram. Soc.*, 1992, **75**, 2420.
13 T. Itoh, *J. Cryst. Growth*, 1992, **125**, 223.
14 S. K. Saka and P. Pramanik, *J. Non-Cryst. Solids*, 1993, **159**, 31.
15 T. Mori, H. Yamamura, H. Kobayashi and T. Mitamura, *J. Mater. Sci.*, 1993, **28**, 4970.
16 T. Itoh, *J. Mater. Sci. Lett.*, 1994, **13**, 1661.
17 Y. Shi, X. X. Huang and D. S. Yan, *J. Eur. Ceram. Soc.*, 1994, **13**, 113.
18 P. Tartaj, J. Sanz, J. Serna and M. Ocana, *J. Mater. Sci.*, 1994, **29**, 6533.
19 T. Itoh, *J. Mater. Sci. Lett.*, 1985, **4**, 431.
20 R. K. Iler, *The Chemistry of Silica*, Wiley, New York, 1979.
21 S. W. Lee and R. A. Condrate, Sr, *J. Mater. Sci.*, 1988, **23**, 2951.
22 S. Hannane, F. Bertin and J. Bouix, *Bull. Soc. Chim. Fr.*, 1990, **127**, 50.
23 E. Ponthieu, E. Payen and J. Grimblot, *J. Non-Cryst. Solids*, 1992, **147–148**, 598.
24 A. Bertoluzza, C. Fagnano, M. A. Morelli, V. Gottardi and M. Guglielmi, *J. Non-Cryst. Solids*, 1982, **48**, 117.
25 J. S. Hartmann, R. L. Millard and E. R. Vance, *J. Mater. Sci.*, 1990, **25**, 2785.
26 M. Magi, E. Lippmaa, A. Samoson, G. Engelmardt and A. R. Grimmer, *J. Phys. Chem.*, 1984, **88**, 1518.
27 S. Mann, C. C. Perry, R. J. P. Williams, C. A. Fyfe, C. G. Gobbi and G. J. Kennedy, *J. Chem. Soc., Chem. Commun.*, 1983, 168.

Paper a906003k